

Molecular effects in the ionization of N₂, O₂, and F₂ by intense laser fields

Daniel Dundas* and Jan M. Rost

Max Planck Institute for the Physics of Complex Systems, Nöthnitzer Strasse 38, 01187 Dresden, Germany

(Received 17 September 2004; published 21 January 2005)

In this paper we study the response in time of N₂, O₂, and F₂ to laser pulses having a wavelength of 390 nm. We find single-ionization suppression in O₂ and its absence in F₂, in accordance with experimental results at $\lambda=800$ nm. Within our framework of time-dependent density functional theory we are able to explain deviations from the predictions of intense-field many-body *S*-matrix theory (IMST). We confirm the connection of ionization suppression with destructive interference of outgoing electron waves from the ionized electron orbital. However, the prediction of ionization suppression, justified within the IMST approach through the symmetry of the highest occupied molecular orbital (HOMO), is not reliable since it turns out that—e.g., in the case of F₂—the electronic response to the laser pulse is rather complicated and does not lead to dominant depletion of the HOMO. Therefore, the symmetry of the HOMO is not sufficient to predict ionization suppression. However, at least for F₂, the symmetry of the dominantly ionized orbital is consistent with the nonsuppression of ionization.

DOI: 10.1103/PhysRevA.71.013421

PACS number(s): 42.50.Hz, 33.80.Eh

I. INTRODUCTION

In the last two decades the interaction of atoms and molecules with intense laser pulses has attracted widespread research. This highly nonperturbative interaction results in a number of nonlinear processes such as ionization, harmonic generation, and above-threshold ionization. At the heart of all these processes is single-electron ionization which gives rise, either directly or indirectly, to the other processes.

Compared to atoms, molecules represent a more complex class of system due to their multicenter nature which introduces additional vibrational and rotational degrees of freedom. It is perhaps surprising therefore that the ionization of molecules by intense laser pulses shares many of the characteristics with the ionization of atoms. The mechanisms of ionization can be characterized as either multiphoton transitions or tunneling ionization, or some combination of both. The process can be classified into either the tunneling or multiphoton regime by the Keldysh parameter, defined as $\gamma_k \equiv \sqrt{I_p}/2U_p$, where the internal binding energy is I_p and the external laser-driven kinetic energy is U_p . In the long-wavelength, the intense field limit $\gamma_k \ll 1$ and tunneling dominates and thus the excited-state spectrum should play no role in the ionization process.

In a range of early experiments this was found to be the case: it was discovered that single-ionization rates for molecules are roughly identical to those of noble-gas atoms provided the ionization potentials were comparable [1–4]. In one of these experiments [4] the single-ionization rates of O₂ ($I_p=12.07$ eV) and of its companion noble-gas atom xenon ($I_p=12.13$ eV) were measured simultaneously by exposing a target containing a mixture of xenon atoms and O₂ to a laser pulse of wavelength $\lambda=10.6$ μm . The ionization rates were found to be similar.

However, in later experiments carried out at Ti:sapphire laser wavelengths ($\lambda \sim 800$ nm) it was found that while most atom-molecule pairs obeyed this finding—such as N₂ ($I_p=15.58$ eV) and its companion atom argon ($I_p=15.76$ eV)—a number did not. For example, the single-ionization rate of O₂ was suppressed with respect to the ionization rate of xenon by several orders of magnitude [5,6] while ionization of D₂ was also suppressed with respect to its companion noble-gas atom, argon.

Considerable interest has been generated by these findings and a number of explanations have been put forward for the origin of the suppression, most notably in O₂. Talebpour *et al.* [5] suggested a dissociative recombination process leading to a decrease in the single-ionization signal. However, later experiments [6] concluded that dissociative recombination cannot be the cause of suppression since the suppression was observed for a range of laser polarization ellipticities. An electronic correction to tunneling theory was suggested by Guo [7] and reproduced the correct suppression of O₂, provided that correct parameters for an effective nuclear charge and ionization potential are chosen.

Muth-Böhm *et al.* [8] explained the suppression of the O₂ single-ionization rate using a generalization of intense-field many-body *S*-matrix theory (IMST) which included an interference term. They showed with their calculations that the suppression of the O₂ signal with respect to xenon—and its absence in N₂/Ar—is due to a symmetry-induced dynamical effect whereby interference between ionizing wave packets emitted from the two distinct nuclear centers is either destructive or constructive in the low-energy limit, depending upon the symmetry of the highest occupied molecular orbital (HOMO). Thus for O₂, in which the HOMO has an antibonding character (ground-state configuration $1\sigma_g^2 1\sigma_u^2 2\sigma_g^2 2\sigma_u^2 3\sigma_g^2 1\pi_u^4 1\pi_g^2$), single ionization should show suppression. For N₂, in which the HOMO has a bonding character (ground-state configuration $1\sigma_g^2 1\sigma_u^2 2\sigma_g^2 2\sigma_u^2 1\pi_u^4 3\sigma_g^2$), single ionization should not be suppressed. In addition, according to the symmetry argument of

*Present address: Max Planck Institute for Nuclear Physics, Saupfercheckweg 1, 69117 Heidelberg, Germany.

IMST, when suppression does occur we can write

$$k_N \cdot \mathbf{R} \ll 1, \quad (1)$$

where $k_N^2/2 = N\omega - U_p - I_p$ is the kinetic energy of the electron on absorbing N photons, ω the laser frequency, and R the bond length of the molecule. Thus, if only the wavelength is varied, the suppression should be enhanced at shorter wavelengths. This explanation is consistent with the O_2/Xe results where suppression of O_2 was observed at $\lambda = 800$ nm but not at $\lambda = 10.6$ μm .

Following the symmetry argument it was postulated that since F_2 ($I_p = 15.69$ eV) has an ionization potential similar to N_2 and argon but has valence electrons with the same symmetry as O_2 (ground-state configuration of F_2 : $1\sigma_g^2 1\sigma_u^2 2\sigma_g^2 2\sigma_u^2 3\sigma_g^2 1\pi_u^4 1\pi_g^4$), ionization of F_2 should also be suppressed with respect to either N_2 or argon [8]. However, a later experimental study [9] showed that the ionization of F_2 is not suppressed with respect to that of N_2 .

In this paper we study the response in time of N_2 , O_2 , and F_2 to laser pulses having a wavelength of 390 and 300 nm. We find single-ionization suppression in O_2 and its absence in F_2 , in accordance with the experimental results at $\lambda = 800$ nm. Within our framework of a time-dependent density functional approach we are able to explain the deviations from the predictions based on the symmetry of the HOMO. The paper is arranged as follows. In Sec. II the time-dependent density functional approach is set out and the procedure for calculating single-ionization rates described. In Sec. III the time evolution will be considered. Finally, some conclusions will be drawn in Sec. IV.

II. METHOD

The time-dependent density functional method provides the most detailed, practical, and feasible *ab initio* approach for tackling many-body problems. Density functional theory (DFT), as first introduced by Hohenberg and Kohn [10] and Kohn and Sham [11], describes a system of interacting particles in terms of its density. The theory is based on the existence of an exact mapping between densities and external potentials and leads to the density of the interacting system being obtained from the density of an auxiliary system of noninteracting particles moving in an effective local single-particle potential; i.e., the particle interactions are treated in an averaged-over manner. A time-dependent formalism of DFT (TDDFT) was provided by Runge and Gross [12], who showed that the time-dependent density could be obtained from the response of noninteracting particles to the time-dependent local effective potential. In principle, many-body effects are included exactly through an exchange-correlation functional; in practice, the form of this functional is unknown and at best it can only be approximated.

Such an approach has been widely used in treating the interaction of molecules with intense, short-duration laser pulses. For instance, in the approach of Chu and Chu [13,14] a pseudospectral mesh technique is used in the solution of the Kohn-Sham equations. A nonadiabatic quantum molecular dynamics (NA-QMD) method, in which the electron dynamics are treated quantum mechanically using TDDFT, has

been developed by Uhlmann *et al.* [16]. In this work the electron orbitals are expanded in terms of Gaussian basis functions. More recently, Castro *et al.* [17] developed grid-based NA-QMD technique to study harmonic generation in H_2 . However, these calculations were limited to a one-dimensional (1D) treatment of the electron dynamics. Another grid-based DFT method has been developed by Otobe *et al.* [15]. While this method has calculated tunnel ionization rates for N_2 , O_2 , and F_2 two approximations have been made. First, a pseudopotential description of the electron-nuclear potential was used, meaning that only the valence electrons in the molecules were treated. Second, only static-field ionization rates were calculated.

The current approach utilizes a NA-QMD approach in which the electron dynamics are described by a hybrid finite-difference-Lagrange-mesh technique [18]. For the present calculations, however, a fixed nuclei description has been employed. Details of the approach are now given.

A. Time-dependent Kohn-Sham equations

In the TDDFT approach, the total N_e -electron Kohn-Sham wave function is written as a single determinant of one-particle Kohn-Sham orbitals. Denoting the spin state of each orbital by the label $\sigma = \uparrow, \downarrow$, we can write the electron density as

$$n(\mathbf{r}, t) = \sum_{\sigma=\uparrow,\downarrow} n_{\sigma}(\mathbf{r}, t) = \sum_{\sigma=\uparrow,\downarrow} \sum_{i=1}^{N_{\sigma}} |\psi_{i\sigma}(\mathbf{r}, t)|^2, \quad (2)$$

where N_{σ} is the number of electrons in spin state σ and $\psi_{i\sigma}(\mathbf{r}, t)$ are the Kohn-Sham orbitals. The orbitals are obtained through the solution of the time-dependent Kohn-Sham equations

$$i \frac{\partial}{\partial t} \psi_{i\sigma}(\mathbf{r}, t) = \left[-\frac{1}{2} \nabla^2 + V_{\text{eff}}(\mathbf{r}, t) \right] \psi_{i\sigma}(\mathbf{r}, t), \quad (3)$$

where

$$V_{\text{eff}}(\mathbf{r}, t) = V_{\text{ext}}(\mathbf{r}, \mathbf{R}, t) + V_H(\mathbf{r}, t) + V_{xc\sigma}(\mathbf{r}, t) \quad (4)$$

is the time-dependent effective potential which is given in terms of the external potential

$$V_{\text{ext}}(\mathbf{r}_i, \mathbf{R}, t) = V_{\text{ions}}(\mathbf{r}_i, \mathbf{R}, t) + U_{\text{elec}}(\mathbf{r}_i, t), \quad (5)$$

where $U_{\text{elec}}(\mathbf{r}_i, t)$ denotes the interaction between electron i and the applied laser field and where

$$V_{\text{ions}}(\mathbf{r}_i, \mathbf{R}, t) = \sum_{I=1}^{N_n} V_{\text{ion}}(\mathbf{r}_i, \mathbf{R}_I, t) = - \sum_{I=1}^{N_n} \frac{Z_I}{|\mathbf{R}_I - \mathbf{r}_i|} \quad (6)$$

denotes the Coulomb interaction between electron i and all ions. The time-dependent effective potential also depends on the Hartree potential

$$V_H(\mathbf{r}, t) = \int d\mathbf{r}' \frac{n(\mathbf{r}', t)}{|\mathbf{r} - \mathbf{r}'|} \quad (7)$$

and the exchange-correlation potential

$$V_{xc\sigma}(\mathbf{r}, t) = \left. \frac{\delta E_{xc}[n_{\uparrow}, n_{\downarrow}]}{\delta n_{\sigma}} \right|_{n_{\sigma}=n_{\sigma}(\mathbf{r}, t)}, \quad (8)$$

where $E_{xc}[n_{\uparrow}, n_{\downarrow}]$ is the exchange-correlation action.

B. Treatment of the exchange-correlation potential

All many-body effects are included within the exchange-correlation potential, which in practice must be approximated. While many sophisticated approximations to this potential have been developed [19], the simplest is the adiabatic local density approximation in the exchange-only limit (xLDA). In this case the exchange energy functional is given by

$$E_x[n_{\uparrow}, n_{\downarrow}] = -\frac{3}{2} \left(\frac{3}{4\pi} \right)^{1/3} \sum_{\sigma=\uparrow, \downarrow} \int d\mathbf{r} n_{\sigma}^{4/3}(\mathbf{r}, t), \quad (9)$$

from which the exchange-correlation potential

$$V_{xc\sigma}(\mathbf{r}, t) = -\left(\frac{6}{\pi} \right)^{1/3} n_{\sigma}^{1/3}(\mathbf{r}, t) \quad (10)$$

can be obtained. This approximate functional is easy to implement and is one of the most widely used exchange-correlation functionals. However, it does suffer from a number of drawbacks; most notably it contains self-interaction errors. This self-interaction means that the asymptotic form of the potential is exponential instead of Coulombic. Therefore, the electronic properties and response of the system can differ markedly from those of the actual system (as we shall see, for example, in Sec. III A).

C. Numerical details

Precise numerical details of how the code is implemented are given in [18]. Briefly, the numerical implementation of TDDFT uses a cylindrical grid treatment of the electronic Kohn-Sham orbitals. A finite-difference treatment of the z coordinate and a Lagrange-mesh treatment of the ρ coordinate based upon Laguerre polynomials is used, similar to that used in previous treatments of H₂⁺ and H₂ [22–25]. For the case of diatomic molecules and considering a linearly polarized laser pulse with the laser polarization direction parallel to the molecular axis the azimuthal angle ϕ can be treated analytically. The time-dependent Kohn-Sham equations of TDDFT are discretized in space using these grid techniques and the resulting computer code parallelized to run on massively parallel processors. Several parameters in the code affect the accuracy of the method. These are the number of points in the finite-difference grid (N_z), the finite-difference grid spacing (Δz), the number of Lagrange-Laguerre mesh points (N_{ρ}), the scaling parameter of the Lagrange-Laguerre mesh (h_{ρ}), the order of the time propagator (N_t), and the time spacing (Δt) [18]. In all the calculations presented here, converged results were obtained using the following parameters (atomic units are used throughout): $N_z=2291$, $\Delta z=0.05$, $N_{\rho}=43$, $h_{\rho}=0.288\ 387\ 71$, $N_t=18$, and $\Delta t=0.02$. The code was parallelized and the calculations were carried out using 79 processors.

D. Determination of ionization

Within TDDFT all observables are functionals of the electronic density. However, as in the case of the exchange correlation functional, the exact forms of these functionals may not be known and must therefore be approximated. The functional describing ionization falls into this category. To date, most calculations of ionization within TDDFT have been obtained using geometric properties of the time-dependent Kohn-Sham orbitals [20]. Briefly, an analyzing box is introduced as a way to approximately separate the bound- and continuum-state parts of the wave function. We define the box such that all relevant bound states of the wave function are contained inside this box while the continuum contributions are found outside the box. In that case the number of bound electrons is given by

$$N_{\text{bound}}(t) = \int_{\text{inside box}} d\mathbf{r} n(\mathbf{r}, t), \quad (11)$$

while the number of continuum electrons is given by

$$N_{\text{esc}}(t) = \int_{\text{outside box}} d\mathbf{r} n(\mathbf{r}, t). \quad (12)$$

We then define the number of bound and continuum electrons for each Kohn-Sham orbital as (dropping spin subscripts)

$$N_j(t) = \int_{\text{inside box}} d\mathbf{r} |\psi_j(\mathbf{r}, t)|^2 \quad (13)$$

for bound electrons and

$$\bar{N}_j(t) = \int_{\text{outside box}} d\mathbf{r} |\psi_j(\mathbf{r}, t)|^2 \quad (14)$$

for continuum electrons. Thus we obtain approximate ion probabilities $P^k(t)$ for the charge state k . In particular we find

$$P^0(t) = N_1(t) \cdots N_{N_e}(t) \quad (15)$$

and

$$P^1(t) = \sum_{n=1}^{N_e} N_1(t) \cdots \bar{N}_n(t) \cdots N_{N_e}(t). \quad (16)$$

III. RESULTS

We now study the response of N₂, O₂, and F₂ to intense laser pulses. First, we compute the ionization potentials of the various molecules. Then we compare single ionization of N₂ and F₂ showing that the F₂⁺ yield shows no suppression with respect to the N₂⁺ yield. Third, we compare the yields of O₂⁺ using two initial configurations of the molecule: namely, a singlet and a triplet state. This shows that the suppression of the O₂⁺ signal is not due to the fact that the O₂ ground state is a triplet configuration. In order to gain a better understanding of the electronic dynamics we analyze the time evolution of the Kohn-Sham orbitals, showing that in the case of F₂ the response of the core electrons shows a significant response to the pulse.

TABLE I. Ionization potentials of N_2 , O_2 , and F_2 calculated using a TDDFT approach within the exchange-only local density approximation compared with the experimental values [26]. While the ionization potentials of N_2 and O_2 agree to within 5%, those for F_2 differ by 10%.

	Ionization potential (eV)		
	N_2	O_2	F_2
Present	15.91	11.45	14.14
Exact	15.58	12.07	15.69

A. Ionization potentials

The starting point for any simulation of the response of diatomic molecules to intense laser pulses is an appropriate description of the field-free structure. In our calculations we assume that the molecules are initially in their ground states. Starting from the equilibrium ion separation the ground-state electronic density is calculated self-consistently from the time-dependent Kohn-Sham equations using an iterative Lanczos method [21,22]. Of particular importance in the present calculations are the ionization potentials of the different molecules. These are obtained by first calculating the ground-state energy of the particular molecule and then that of the molecule with one electron removed. The results are presented in Table I for N_2 , O_2 , and F_2 . We see that the ionization potentials of N_2 and O_2 compare well to the experimental values [26] while the ionization potential of F_2 shows a 10% difference with the experimental value. The difference can be explained in terms of the choice of exchange-correlation potential, as discussed earlier. Obviously in comparing single ionization in N_2 and F_2 the errors in their ionization potentials will have an important impact upon their subsequent response. It has been pointed out to us [27] that the 10% decrease in the ionization potential of F_2 could increase the single-ionization yield by two orders of magnitude. However, such an estimation, obtained using IMST, only takes into account the response of the HOMO to the field. As our results will show, it appears that molecular effects due to the other orbitals are extremely important in this system and such a large increase in ionization yield due to a lowering of the ionization potential is unlikely. This is supported by the static-field tunnel ionization calculations of Otobe *et al.* [15] who employed a DFT approach using the self-interaction free *KLI* approximation. In these calculation the ionization potential of F_2 was much closer to the experimental value. However, no suppression of the F_2^+ signal was evident.

B. Single-ionization yields of N_2 and F_2

Table II presents a comparison of the single-ionization yields for N_2^+ and F_2^+ after the interaction of the neutral molecules with a 24-cycle laser pulse (pulse length, $\tau = 31.2$ fs) having a wavelength of $\lambda = 390$ nm over the intensity range $I = 1 - 8 \times 10^{14}$ W/cm². As discussed in the Introduction, if the symmetry-induced dynamical effect is responsible for ionization suppression, Eq. (1) predicts that the

TABLE II. Ion yields of N_2^+ and F_2^+ after interaction of the neutral molecules with a 24-cycle laser pulse having a wavelength of $\lambda = 390$ nm for a range of laser intensities. The ion yields differ by factor of less than 3. Hence, the F_2^+ yield is not suppressed with respect to the N_2^+ yield.

Laser intensity (10^{14} W/cm ²)	Ion yields	
	N_2^+	F_2^+
1.0	0.2479176	0.1051454
2.0	0.3804471	0.2523075
4.0	0.4025715	0.3742050
6.0	0.3501940	0.3278126
8.0	0.2919808	0.3375370

yield of F_2^+ ions should be suppressed to a greater extent to the yield of N_2^+ ions at the wavelength used in these calculations. While differences do exist between the N_2^+ and F_2^+ ion yields, we see that the differences are no more than a factor of 3. We conclude that *single ionization of F_2 is not suppressed with respect to the single ionization of N_2 .*

C. Single-ionization yields from 1O_2 and 3O_2

One explanation postulated for the nonatomiclike single ionization in O_2 compared to single ionization of N_2 is the fact that the ground state of O_2 is a triplet state with a half-filled open-shell structure whereas the ground state of N_2 is a singlet state with a closed-shell structure [6]. Muth-Böhm *et al.* [8] argued that such a difference in the spin states is unlikely to influence the ionization signal since the spin degrees of freedom are not effectively coupled to a dipole field. We are unaware of any calculation to date in which single ionization of O_2 is studied as a function of the multiplicity of the ground state.

Table III compares the single-ionization yields of 1O_2 and 3O_2 at the end of a 24-cycle laser pulse ($\tau = 31.2$ fs) having a wavelength of $\lambda = 390$ nm over the intensity range $I = 1 - 8 \times 10^{14}$ W/cm². We see that no significant difference of the yields due to the two configurations is evident. Hence, we

TABLE III. Ion yields of O_2^+ (assuming either an initial singlet or triplet configuration of the neutral O_2 molecule) after interaction with a 24-cycle laser pulse having a wavelength of $\lambda = 390$ nm for a range of laser intensities. The ion yields roughly agree, indicating that the multiplicity of the ground state of O_2 does not play a role in the suppression of the O_2^+ yield.

Laser intensity (10^{14} W/cm ²)	Ion yield	
	$^1O_2 \rightarrow O_2^+$	$^3O_2 \rightarrow O_2^+$
1.0	0.0009385	0.0006335
2.0	0.0022583	0.0017794
4.0	0.0038756	0.0032043
6.0	0.0041731	0.0033902
8.0	0.0036198	0.0027161

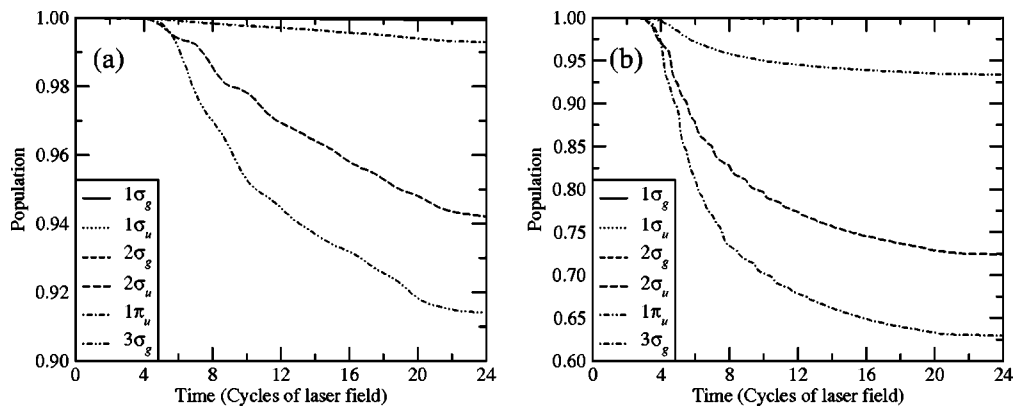


FIG. 1. Kohn-Sham orbital populations for N₂ during interaction with a 24-cycle laser pulse having a wavelength of $\lambda=390$ nm and laser intensity (a) $I=1 \times 10^{14}$ W/cm² and (b) $I=6 \times 10^{14}$ W/cm². For all laser intensities it is seen that the Kohn-Sham orbital having the same symmetry ($3\sigma_g$) as the valence orbital of N₂ shows the predominant response to the field.

conclude that the *suppression of O₂⁺ with respect to that of Xe⁺ is not due to the ground state of O₂ being a triplet state.*

D. Orbital response of N₂, O₂, and F₂

In order to gain a better understanding of the ionization dynamics we have investigated the time evolution of the Kohn-Sham orbitals. It must be stressed that these orbitals do not have any physical significance with the molecular orbitals of the actual system. However, studying the evolution of the Kohn-Sham orbitals allows us to obtain information about the orbital symmetries. In Fig. 1 we present results for the time evolution of the Kohn-Sham orbitals of N₂ during its interaction with a 24-cycle laser pulse of wavelength $\lambda=390$ nm. Two laser intensities are presented: $I=1 \times 10^{14}$ W/cm² and $I=6 \times 10^{14}$ W/cm². It can clearly be seen that the orbital having the same symmetry ($3\sigma_g$) as the valence orbital of N₂ shows the dominant response to the field. The same behavior is observed for all other laser intensities considered in Table II. Thus it is apparent that single ionization of N₂ occurs predominantly by ionization of the valence electron. Since the valence orbital of N₂ has a bonding character, then, based upon the symmetry arguments of IMST, we

would expect no ionization suppression to occur—as is the case.

In Fig. 2 we present results for the time evolution of the Kohn-Sham orbitals of O₂ during its interaction with a 24-cycle laser pulse of wavelength $\lambda=390$ nm. Again, two laser intensities are presented: $I=1 \times 10^{14}$ W/cm² and $I=6 \times 10^{14}$ W/cm². As in the case of N₂ we see that the orbital having the same symmetry ($1\pi_g$) as the valence orbital of O₂ shows the dominant response to the field and thus single ionization of O₂ occurs predominantly by ionization of the valence electron. Since the valence orbital of O₂ has an antibonding character, then, based upon the symmetry argument of IMST, we would expect ionization suppression to occur—again, in accordance with the numerical results and experiment.

In Fig. 3 we present results for the time evolution of the Kohn-Sham orbitals of F₂ during its interaction with a 24-cycle laser pulse of wavelength $\lambda=390$ nm. Four laser intensities are presented: $I=1 \times 10^{14}$ W/cm², $I=2 \times 10^{14}$ W/cm², $I=4 \times 10^{14}$ W/cm², and $I=6 \times 10^{14}$ W/cm². It is apparent that the orbital having the same symmetry ($1\pi_g$) as the valence orbital of F₂ does not in this case show the dominant response to the field. Instead we see that for all of the intensities, apart from $I=1 \times 10^{14}$ W/cm², the orbital

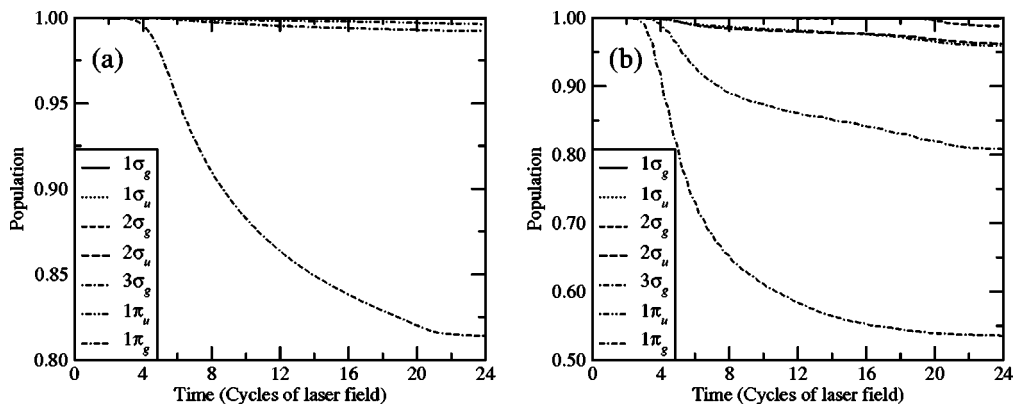


FIG. 2. Kohn-Sham orbital populations for O₂ during interaction with a 24-cycle laser pulse having a wavelength of $\lambda=390$ nm and laser intensity (a) $I=1 \times 10^{14}$ W/cm² and (b) $I=6 \times 10^{14}$ W/cm². For all laser intensities it is seen that the Kohn-Sham orbital having the same symmetry ($1\pi_g$) as the valence orbital of O₂ shows the predominant response to the field.

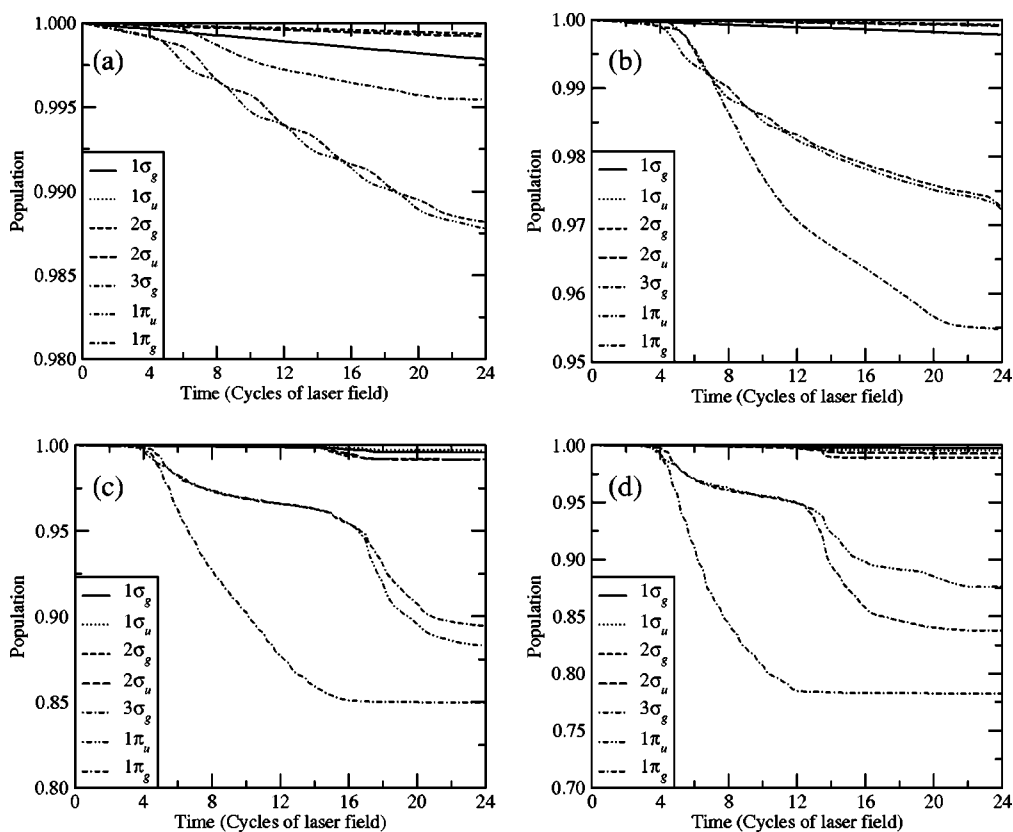


FIG. 3. Kohn-Sham orbital populations for F_2 during interaction with a 24-cycle laser pulse having a wavelength of $\lambda=390$ nm and laser intensity (a) $I=1 \times 10^{14}$ W/cm 2 , (b) $I=2 \times 10^{14}$ W/cm 2 , (c) $I=4 \times 10^{14}$ W/cm 2 , and (d) $I=6 \times 10^{14}$ W/cm 2 . For all laser intensities, except $I=1 \times 10^{14}$ W/cm 2 , it is seen that the $3\sigma_g$ orbital predominantly responds to the field. At the lowest intensity the $1\pi_g$ antibonding orbital (having the same symmetry as the valence orbital of F_2) is equally dominant with the $1\pi_u$ bonding orbital. These two orbitals respond almost identically at all laser intensities.

having the symmetry $3\sigma_g$ shows the dominant response. Since this orbital has a bonding character, then, based upon the predictions of IMST, ionization suppression will not occur. We conclude that single ionization of F_2 does not occur predominantly by ionization of the valence electron. Thus, molecular structure effects for this molecule are of crucial importance.

In understanding why the orbital having the same symmetry ($1\pi_g$) as the valence orbital of F_2 does not respond predominantly to the field we consider the response of F_2 at the laser intensity of $I=1 \times 10^{14}$ W/cm 2 where the $3\sigma_g$ orbital did not show the dominant response to the field. In this case the $1\pi_g$ antibonding orbital and the $1\pi_u$ bonding orbital showed the dominant response. Indeed we see that over all laser intensities these two orbitals respond in a similar fashion to the field. It would therefore appear that an interference is occurring between these two orbitals.

To gain further insight we have repeated the TDDFT calculations at the laser intensity of $I=2 \times 10^{14}$ W/cm 2 , whereby only a subset of the orbitals was allowed to respond to the field, all other orbitals being frozen. The results are presented in Fig. 4. We see from Fig. 4(c) that when only the $1\pi_u$ and $1\pi_g$ orbitals respond to the field is ionization suppressed. In Figs. 4(a) and 4(b) we see that the ionization of either the $1\pi_u$ or $1\pi_g$ is greater than that of the $3\sigma_g$ orbital. In Fig. 4(d), when the $3\sigma_g$, $1\pi_u$, and $1\pi_g$ orbitals respond,

ionization of the $3\sigma_g$ is dominant. This behavior illustrates a rather complicated correlated response of the orbitals to the laser field. Moreover, from Fig. 3 we can see that a resonance effect is coming into play. This is evidenced at the laser intensities of $I=4 \times 10^{14}$ W/cm 2 and $I=6 \times 10^{14}$ W/cm 2 where the rate of depletion of the $1\pi_u$ and $1\pi_g$ orbitals is not exponential but instead shows evidence of two distinct rates being present: namely, an intermediate resonance state is initially populated and then undergoes ionization itself. Figure 5 presents results for the time evolution of the Kohn-Sham orbitals of F_2 during its interaction with a 24-cycle laser pulse of wavelength $\lambda=300$ nm at laser intensities $I=4 \times 10^{14}$ W/cm 2 and $I=6 \times 10^{14}$ W/cm 2 . In this case the orbital populations are depleted exponentially, thus confirming the presence of the resonance at $\lambda=390$ nm.

Hence, we confirm the connection of the suppression of ionization with destructive interference of outgoing electron waves from the ionized electron orbital as put forward first by Muth-Böhmer *et al.* [8]. However, the prediction of ionization suppression justified within the IMST approach through the symmetry of the HOMO is not reliable, since it turns out that, e.g., in the case of F_2 the electronic response to the laser pulse is rather complicated and does not lead to dominant depletion of the HOMO. Therefore, the symmetry of the HOMO is not sufficient to predict ionization suppression. However, at least for F_2 , the symmetry of the dominantly

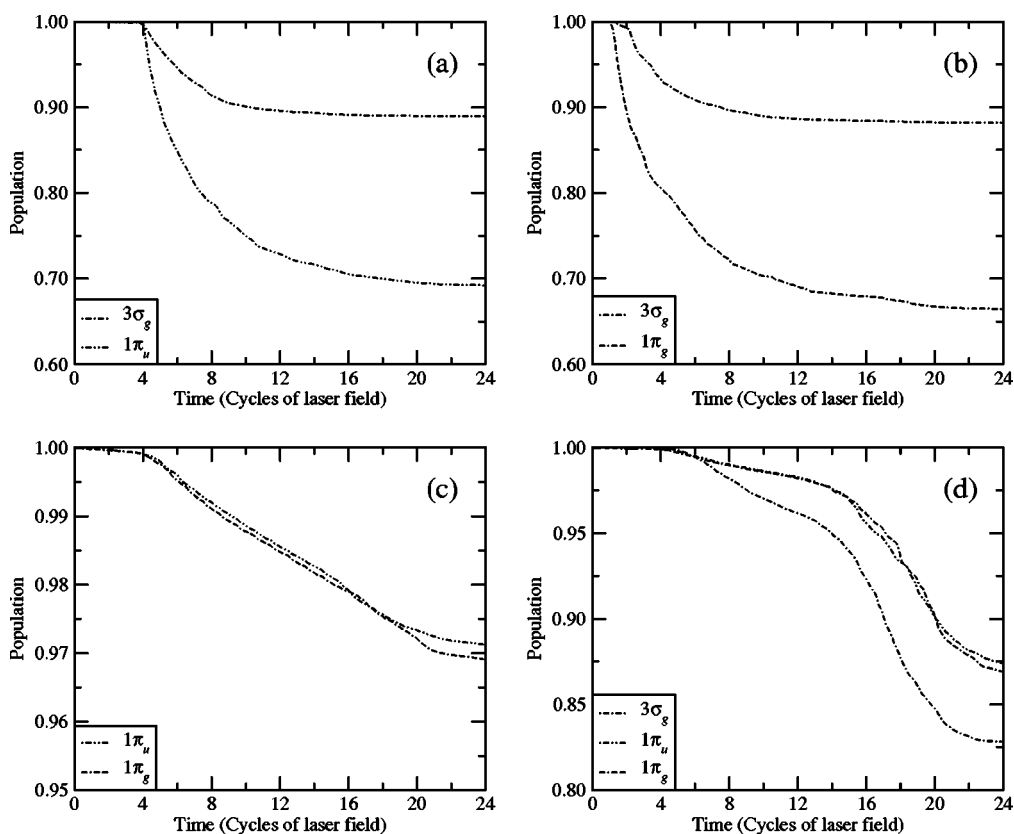


FIG. 4. Kohn-Sham orbital populations for F₂ during interaction with a 24-cycle laser pulse having a wavelength of $\lambda=390$ nm and an intensity of $I=2 \times 10^{14}$ W/cm². In these calculations only the orbitals shown in each figure respond to the field. All other orbitals are frozen. It can clearly be seen in (c) that when only the $1\pi_u$ and $1\pi_g$ orbitals respond to the field is ionization suppressed. In (a) and (b) we see that the ionization of either the $1\pi_u$ or $1\pi_g$ is greater than that of the $3\sigma_g$ orbital. When the $3\sigma_g$, $1\pi_u$, and $1\pi_g$ orbitals respond, however, ionization of the $3\sigma_g$ orbital is dominant.

ionized orbital is consistent with the nonsuppression of ionization.

IV. SUMMARY

Single ionization of N₂, O₂, and F₂ by intense laser fields having a wavelength of $\lambda=390$ nm has been simulated using

a time-dependent density functional approach within the exchange-only local density approximation. The results obtained for the single ionization of N₂ and O₂ are in agreement with IMST results [8] if the HOMO is dominantly ionized. This is the case for N₂ and O₂, where for the latter molecule destructive interference leads to a suppression of

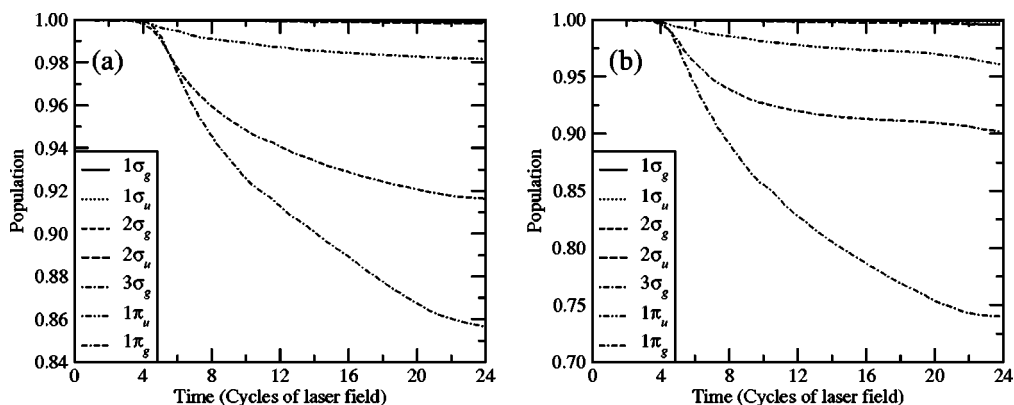


FIG. 5. Kohn-Sham orbital populations for F₂ during interaction with a 24-cycle laser pulse having a wavelength of $\lambda=300$ nm and intensity (a) $I=4 \times 10^{14}$ W/cm² and (b) $I=6 \times 10^{14}$ W/cm². At this laser wavelength we see that the the orbital populations fall off exponentially, unlike the response at $\lambda=390$ nm observed in Fig. 3. We conclude that the response at $\lambda=390$ nm is due to the population of an intermediate resonance state.

ionization. In addition it is found that the suppressed ionization of O_2 with respect to its companion noble-gas atom (xenon) does not arise from the multiplicity of the ground state of O_2 .

For single ionization of F_2 , it is found that the ionization signal is not suppressed with respect to the N_2^+ yield, in keeping with other static-field TDDFT results [15]. Multi-electron molecular correlation leads to the dominant ionization of an orbital with symmetry different from the one of the HOMO. This is the reason why the prediction based on the symmetry of the HOMO fails [8].

The present calculations are carried out within xLDA. Implementations of TDDFT which go beyond the xLDA approximation to a self-interaction free exchange-correlation potential improve the description of the ionization potentials

and will be the focus of future work. In addition only parallel transition have been considered in this paper which is a reasonable approximation for strong-field ionization of diatomics. Future work will focus on generalizing the calculations of single-ionization rates to arbitrary orientations between the molecular axis and the laser polarization direction.

ACKNOWLEDGMENTS

The authors would like to acknowledge useful discussions with Andreas Becker. The work reported in this paper is supported by the UK Engineering and Physical Sciences Research Council by provision of computer resources at Computer Services for Academic Research, University of Manchester and HPC(X), Daresbury Laboratory.

-
- [1] G. N. Gibson, R. R. Freeman, and T. J. McIlrath, *Phys. Rev. Lett.* **67**, 1230 (1991).
- [2] S. L. Chin, Y. Liang, J. E. Decker, F. A. Ilkov, and M. V. Ammosov, *J. Phys. B* **25**, L249 (1992).
- [3] T. D. G. Walsh, J. E. Decker, and S. L. Chin, *J. Phys. B* **26**, L85 (1993).
- [4] T. D. G. Walsh, F. A. Ilkov, J. E. Decker, and S. L. Chin, *J. Phys. B* **27**, 3767 (1994).
- [5] A. Talebpour, C.-Y. Chien, and S. L. Chin, *J. Phys. B* **29**, L677 (1996).
- [6] C. Guo, M. Li, J. P. Nibarger, and G. N. Gibson, *Phys. Rev. A* **58**, R4271 (1998).
- [7] C. Guo, *Phys. Rev. Lett.* **85**, 2276 (2000).
- [8] J. Muth-Böhm, A. Becker, and F. H. M. Faisal, *Phys. Rev. Lett.* **85**, 2280 (2000).
- [9] M. J. DeWitt, E. Wells, and R. R. Jones, *Phys. Rev. Lett.* **87**, 153001 (2001).
- [10] P. Hohenberg and W. Kohn, *Phys. Rev.* **136**, B864 (1964).
- [11] W. Kohn and L. J. Sham, *Phys. Rev.* **140**, A1133 (1965).
- [12] E. Runge and E. K. U. Gross, *Phys. Rev. Lett.* **52**, 997 (1984).
- [13] X. Chu and S.-I. Chu, *Phys. Rev. A* **63**, 023411 (2001).
- [14] X. Chu and S.-I. Chu, *Phys. Rev. A* **64**, 063404 (2001).
- [15] T. Otobe, K. Yabana, and J.-I. Iwata, *Phys. Rev. A* **69**, 053404 (2004).
- [16] M. Uhlmann, T. Kunert, F. Grossmann, and R. Schmidt, *Phys. Rev. A* **67**, 013413 (2003).
- [17] A. Castro, M. A. L. Marques, J. A. Alonso, G. F. Bertsch, and A. Rubio, *Eur. Phys. J. D* **28**, 211 (2004).
- [18] D. Dundas, *J. Phys. B* **37**, 2883 (2004).
- [19] J. Kohanoff and N. Gidopoulos, in *Handbook of Molecular Physics and Quantum Chemistry*, edited by S. Wilson (Wiley, Chichester, 2003).
- [20] C. A. Ullrich, *J. Mol. Struct.: THEOCHEM* **501**, 315 (2000).
- [21] E. S. Smyth, J. S. Parker, and K. T. Taylor, *Comput. Phys. Commun.* **114**, 1 (1998).
- [22] D. Dundas, *Phys. Rev. A* **65**, 023408 (2002).
- [23] L.-Y. Peng, D. Dundas, J. F. McCann, K. T. Taylor, and I. D. Williams, *J. Phys. B* **36**, L295 (2003).
- [24] L.-Y. Peng, J. F. McCann, D. Dundas, K. T. Taylor, and I. D. Williams, *J. Chem. Phys.* **120**, 10046 (2004).
- [25] D. Dundas, K. J. Meharg, J. F. McCann, and K. T. Taylor, *Eur. Phys. J. D* **26**, 51 (2003).
- [26] K. P. Huber and G. Herzberg, in *NIST Chemistry WebBook*, edited by P. J. Lindstrom and W. G. Mallard (National Institute of Standards and Technology, Gaithersburg, MD, 2003), Vol. 69.
- [27] A. Becker (private communication).